Radiology

Blood-Brain Barrier Opening with MRI-guided Focused Ultrasound Elicits Meningeal Venous Permeability in Humans with Early Alzheimer Disease

Rashi I. Mehta, MD • Jeffrey S. Carpenter, MD • Rupal I. Mehta, MD • Marc W. Haut, PhD • Manish Ranjan, MD • Umer Najib, MD • Paul Lockman, PhD • Peng Wang, PhD • Pierre-François D'haese, PhD • Ali R. Rezai, MD

From the Departments of Neuroradiology (Rashi I. Mehta, J.S.C., P.W., P.F.D.), Radiology (Rashi I. Mehta, J.S.C.), and Neuroscience (Rashi I. Mehta, J.S.C., M.W.H., P.L., A.R.R.); Rockefeller Neuroscience Institute (Rashi I. Mehta, J.S.C., M.W.H., M.R., U.N., P.L., P.W., P.F.D., A.R.R.); and Departments of Behavioral Medicine and Psychiatry (M.W.H.), Neurosurgery (M.W.H., M.R., A.R.R.), Neurology (M.W.H., U.N.), and Pharmaceutical Sciences (P.L.), West Virginia University, 1 Medical Center Dr, Morgantown, WV 26505; Center for Translational Neuromedicine, University of Rochester, Rochester, NY (Rupal I. Mehta); and Alzheimer's Disease Center and Department of Pathology, Rush University Medical Center, Chicago, Ill (Rupal I. Mehta). Received February 21, 2020; revision requested May 5; revision received September 23; accepted October 30. **Address correspondence to** Rashi I. Mehta (e-mail: *Rashi.Mehta@hsc.wvu.edu*).

Rashi I. Mehta supported by the National Institute of General Medical Sciences of the National Institutes of Health (award 5U54GM104942-04). Rupal I. Mehta supported by the National Institute of Neurological Disorders and Stroke (award K08NS089830).

Conflicts of interest are listed at the end of this article.

See also the editorial by Klibanov in this issue.

Radiology 2021; 298:654–662 • https://doi.org/10.1148/radiol.2021200643 • Content codes: NR MR

Background: Opening of the blood-brain barrier (BBB) induced with MRI-guided focused ultrasound has been shown in experimental animal models to reduce amyloid-β plaque burden, improve memory performance, and facilitate delivery of therapeutic agents to the brain. However, physiologic effects of this procedure in humans with Alzheimer disease (AD) require further investigation.

Purpose: To assess imaging effects of focused ultrasound–induced BBB opening in the hippocampus of human participants with early AD and to evaluate fluid flow patterns after BBB opening by using serial contrast-enhanced MRI.

Materials and Methods: Study participants with early AD recruited to a Health Insurance Portability and Accountability Act–compliant, prospective, ongoing phase II clinical trial (ClinicalTrials.gov identifier, NCT03671889) underwent three separate focused ultrasound–induced BBB opening procedures that used a 220-kHz transducer with a concomitant intravenous microbubble contrast agent administered at 2-week intervals targeting the hippocampus and entorhinal cortex between October 2018 and May 2019. Posttreatment effects and gadolinium-based contrast agent enhancement patterns were evaluated by using 3.0-T MRI.

Results: Three women (aged 61, 72, and 73 years) consecutively enrolled in the trial successfully completed repeated focused ultrasound–induced BBB opening of the hippocampus and entorhinal cortex. Postprocedure contrast enhancement was clearly identified within the targeted brain volumes, indicating immediate spatially precise BBB opening. Parenchymal enhancement resolved within 24 hours after all treatments, confirming BBB closure. Transient perivenous enhancement was consistently observed during the acute phase after BBB opening. Notably, contrast enhancement reappeared in the perivenular regions after BBB closure. This imaging marker is consistent with blood-meningeal barrier permeability and persisted for 24–48 hours before spontaneous resolution. No evidence of intracranial hemorrhage or other adverse effect was identified.

Conclusion: MRI-guided focused ultrasound–induced blood-brain barrier opening was safely performed in the hippocampi of three participants with Alzheimer disease without any adverse effects. Posttreatment MRI reveals a unique spatiotemporal contrast enhancement pattern that suggests a perivenular immunologic healing response downstream from targeted sites.

Online supplemental material is available for this article.

Alzheimer disease (AD) is the most common neurodegenerative disorder and the sixth leading cause of death in the United States (1,2). Despite its devastating health, social, and financial consequences, there is no known treatment and its prevalence continues to increase globally (1). Amyloid-β plaques and neurofibrillary tangles, the pathologic hallmarks of this condition, are associated with chronic neuroinflammation and progressive neuronal and synaptic loss (3). Although reduction of extracellular plaque load has been a primary therapeutic target, numerous failed drug trials highlight the need for innovative approaches to AD therapy (4,5).

MRI-guided focused ultrasound is an innovative technology that uses convergent ultrasound beams to deliver acoustic energy to tissues in a targeted approach. Animal models have demonstrated that focused ultrasound using a low-frequency transducer in combination with an intravascular microbubble contrast agent can cause a transitory opening in the blood-brain barrier (BBB). BBB opening is thought to occur via acoustic cavitation forces with resultant microbubble oscillation and mechanically induced interendothelial tight junction disruption within capillary walls. In rodents, use of this technology has resulted in reduced amyloid-β plaque burden and improved memory performance and has also allowed for targeted drug and stem cell delivery across the BBB (6–10).

Investigations regarding in vivo effects of focused ultrasound–induced BBB opening in experimental models

Abbreviations

AD = Alzheimer disease, BBB = blood-brain barrier, FLAIR = fluid-attenuated inversion recovery

Summary

MRI-guided focused ultrasound–induced blood-brain barrier opening causes meningeal venous permeability manifesting as a temporally evolving contrast enhancement pattern surrounding draining veins in individuals with early Alzheimer disease.

Key Results

- MRI-guided focused ultrasound–induced blood-brain barrier (BBB) opening was safely and effectively achieved in the hippocampi of three individuals with early Alzheimer disease.
- Post-BBB opening MRI showed perivenous contrast agent pooling, suggesting movement of the contrast tracer along the glymphatic efflux pathway.
- An MRI pattern of transient perivenous blood–meningeal barrier permeability was identified and suggests an immunologic healing response.

and individuals living with AD remain limited. We performed the current study given the documented beneficial outcomes in preclinical models (6–10), as well as results of a recent phase I clinical trial (11). The aim of this investigation was to evaluate imaging results and fluid movement patterns after focused ultrasound–induced opening of the BBB targeting the hippocampus and entorhinal cortex, through use of serial contrast-enhanced MRI, to better understand physiologic effects of this treatment in patients with AD.

Materials and Methods

A prospective phase II clinical trial was initiated at our tertiary academic medical center (Rockefeller Neuroscience Institute of West Virginia University) according to a protocol approved by the U.S. Food and Drug Administration and local institutional review board (ClinicalTrials.gov identifier, NCT03671889). This ongoing trial is sponsored by Insightec. Written informed consent was obtained from each participant enrolled in this Health Insurance Portability and Accountability Act–compliant study. Data generated or analyzed during the study are available from the corresponding author by request.

Study Participants

Three women, aged 61, 72, and 73 years, were enrolled consecutively as the first three trial participants after meeting study eligibility requirements. Inclusion criteria included early AD diagnosed with National Institute on Aging–Alzheimer's Association criteria (12), fluorine 18 [^{18}F] florbetaben PET positivity for amyloid-β plaques, and lack of other known central nervous system disease. Additional inclusion and exclusion criteria are listed in Table E1 (online). Participant accrual began in September 2018. Patient enrollment and follow-up are ongoing.

MRI-guided Focused Ultrasound Protocol

Baseline pre- and postcontrast 3.0-T MRI data were acquired 1 week before treatment (Table E2 [online]). Multiple 5 × 5 × 7-mm target volumes and treatment laterality were selected before sonication based on individual anatomy and safety considerations at baseline MRI.

Each study participant underwent three successive sonication sessions, administered at 2-week intervals. The right hippocampus and entorhinal cortex were treated in participant 1, whereas the left hippocampus and entorhinal cortex were treated in participants 2 and 3. Each treatment session consisted of stereotactic headframe placement after head shaving and administration of local anesthesia. Participants were placed in the supine position, with the ExAblate 4000 low-frequency type 2 system helmet transducer (Insightec), consisting of 1024 phased-array elements with a frequency of 220 kHz, positioned over the head. The transducer was integrated with a clinical 3.0-T MRI unit (Signa Architect; GE Healthcare). After intravenous administration of perflutren microbubble contrast material (Definity; Lantheus Medical Imaging), 5 × 5 × 7-mm target volumes were sonicated. Each target volume consisted of a 2 × 2 grid of sonication sites. Each sonication site received 2.6-msec pulses spaced by 30.4 msec for a total of 10 cycles. A 1550-msec rest period followed sonication of all four sites within a target volume. This cycle was then repeated for a total of 90 seconds. The ultrasound power output varied between 4 W and 11.5 W during each 90-second sonication. Selection of the power setting was based on passive acoustic monitoring of cavitation via dedicated hydrophones within the ultrasound assembly during a ramped power test performed 30–40 seconds after initiation of the perflutren injection. The power selected was between 50% and 60% of the ramped power setting that induced subharmonic band acoustic spectra (cavitation halt). Treatment at each target varied between 90 seconds and 270 seconds according to a cavitation score obtained by integrating the acoustic spectra return along a predefined range of frequencies. Peak negative pressures achieved during sonication are estimated to be between 500–1000 kPa.

A total of three target volumes were treated in participants 1 and 2, whereas four target volumes were sonicated in participant 3. The same sites were retreated during the second and third sessions, administered 2 and 4 weeks, respectively, after the initial procedure. Participants were monitored for 24 hours after each therapy, and as of this writing were monitored clinically for up to 19 months after completion of therapy with periodic formal neurologic and neuropsychologic assessments.

Posttreatment MRI Protocol

Posttreatment MRI of the brain was conducted with the same 3.0-T Signa Architect GE MRI unit (GE Healthcare) by using a 48-channel head coil. Pre- and postcontrast MRI of the brain was performed immediately after completion of each sonication session and again at 24 hours after treatment, as well as at 48 hours after treatment for participants 1 and 2. Follow-up brain MRI was also performed 1 week after completion of the final (third) treatment session for each participant, 5 weeks after initial focused ultrasound therapy. MRI sequences acquired included T2* gradient-echo sequences, diffusion, T2-weighted, T2-weighted fluid-attenuated inversion recovery (FLAIR), and pre- and postcontrast T1-weighted sequences with parameters as detailed in Table E2 (online). Serial posttreatment MRI examinations were compared with pre- and postcontrast baseline MRI data. Treated and con-

tralateral (untreated) hippocampal and entorhinal cortex were segmented on baseline and posttreatment MRI scans by using Cranial Suite software (version 5.7; Neurotargeting), and volumetric measurements of these structures were acquired. In addition, precontrast T1 signal intensity of treated volumes was assessed on posttreatment images and compared with baseline data and untreated brain regions. Gadobutrol (0.1 mmol per kilogram of body weight; Bayer Healthcare Pharmaceuticals), administered intravenously, was used as a contrast agent for all MRI studies. The administration of perflutren microbubble contrast material followed the dilute bolus technique, wherein 4 μL/kg was added to preservative-free saline to an approximate volume of 10 mL. This perflutren bolus was administered intravenously over 30 seconds, followed by a 10-mL flush of preservative-free saline.

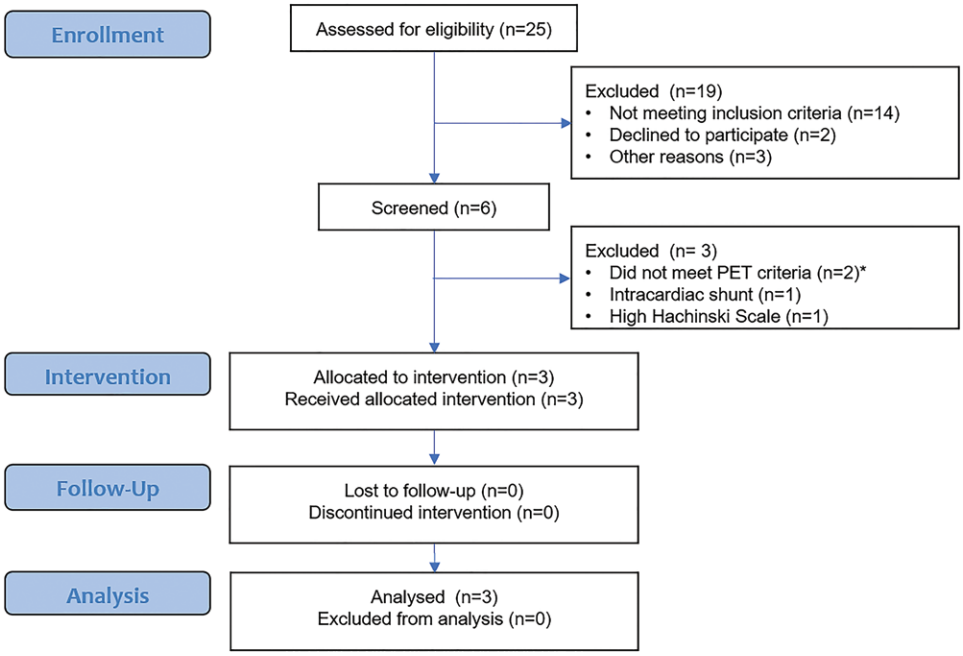

Figure 1: Clinical trial flow diagram.

MRI Analysis

Image analysis was independently conducted by two neuroradiologists (Rashi I. Mehta and J.S.C., with 10 years and 20 years, respectively, of posttraining clinical experience). Analyses were conducted immediately after each MRI acquisition and included assessment for the presence or absence and location of the following: parenchymal enhancement, extraparenchymal enhancement, parenchymal hemorrhage, extraparenchymal hemorrhage, restricted diffusion, parenchymal T2-weighted FLAIR signal hyperintensity, and mass effect. Both readers concurred on diagnostic findings and interpretations.

Results

Participant Characteristics

Twenty-five patients were assessed for study eligibility (Fig 1). Among these, 19 were excluded because they did not meet study inclusion criteria (n = 14), declined to participate (n = 2), or had other logistic reasons for exclusion (n = 3). The remaining six patients underwent screening. Among these, three were excluded because they did not meet PET inclusion criteria (n = 2), had an intracardiac shunt (n = 1), or had a high Hachinski scale score (n = 1). The study population for this analysis consisted of three participants (mean age, 69 years; all women [100%]). Table provides details on additional participant characteristics.

Participant Characteristics

Participant No.	Age (y)	Sex	Time since AD Symptom Onset (y)	MMSE Score
1	61	Female	7	23
2	73	Female	2.5	23
3	72	Female	3	23

Note.—AD = Alzheimer disease, MMSE = Mini–Mental State Examination.

Transient Reversible BBB Opening Was Consistently Achieved

Contrast extravasation was identified within the treated brain volumes immediately after completion of all sonication treatments, indicating focal spatially precise BBB opening within the targeted hippocampi and entorhinal cortex (Fig 2). MRI repeated 24 hours later revealed resolution of parenchymal contrast enhancement at all treated sites, with return of baseline T1 signal intensity and no evidence of new parenchymal enhancement after repeated administration of gadolinium-based contrast agent. This enabled confirmation of BBB closure and expected clearance of interstitial contrast agent within 24 hours at all treated sites.

Extraparenchymal Perivenular Enhancement Was Seen Immediately after BBB Opening

In addition to parenchymal enhancement, a perivascular pattern of enhancement, as shown in Figure 3, was also identified along the course of draining venous structures immediately after sonication treatments. This was shown in the hippocampal fissure, along the course of the intrahippocampal and hippocampal sulcal veins (Fig 3), and was seen longitudinally along the course of these venous structures to the junction with the basal vein of Rosenthal, where ringlike enhancement was seen around the vein (Fig 3, *G*). Similar findings were identified along draining cortical veins in the collateral sulcus in participants 2 and 3. This pattern was best visualized with the postcontrast

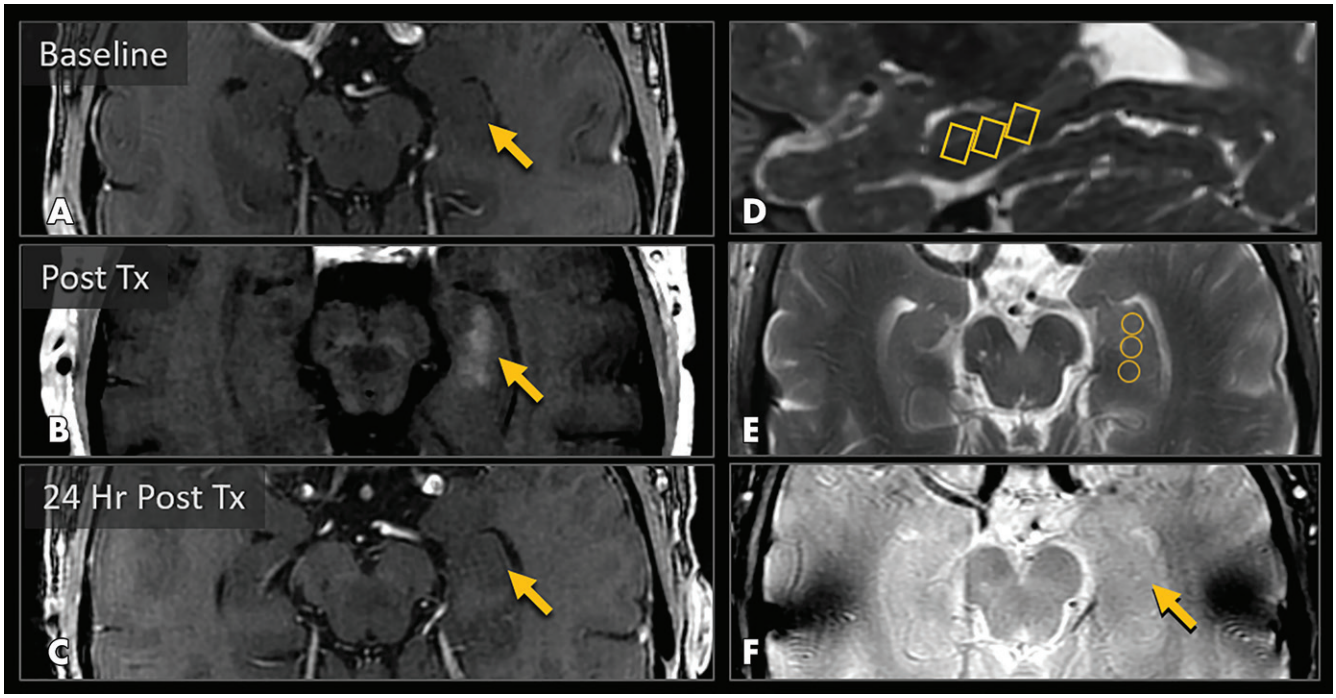

Figure 2: MRI scans show blood-brain barrier (BBB) opening and closure within targeted brain volumes in a 73-year-old woman with Alzheimer disease. Postcontrast T1-weighted images at, *A*, baseline, *B*, immediately after treatment (Tx), and, *C*, 24 hours after treatment show parenchymal contrast material extravasation (arrow in *B*) due to BBB opening locally at the treatment sites and BBB closure with resolution of parenchymal contrast enhancement on repeat gadobutrol administration 24 hours later (arrow in *C*). *D*, Sagittal T2-weighted image shows three 5 × 5 × 7-mm target volumes demarcating the treated areas within the hippocampus and entorhinal cortex. *E*, Target sites shown on axial T2-weighted image. *F*, Axial image obtained with the T2* gradient-echo sequence immediately after treatment shows no evidence of signal dropout to suggest hemorrhage at the treated areas.

FLAIR sequence (Fig 3, *D*), which has high sensitivity to low concentrations of subarachnoid contrast agent and, unlike postcontrast T1-weighted imaging, does not demonstrate parenchymal enhancement.

Perivenular Enhancement Was Observed after BBB Closure after Interstitial and Perivascular Clearance of Gadolinium-based Contrast Agent

Precontrast T1-weighted images at 24 hours after treatment revealed resolution of parenchymal and extraparenchymal contrast enhancement at all treated sites (Fig 4, *C*), indicating rapid clearance of gadobutrol from the interstitial and perivascular spaces after BBB closure. No evidence of contrast agent retention was identified within either of these compartments. After repeated intravenous contrast agent administration at 24 hours after treatment, enhancement was observed in the perivenular region but not in the brain parenchyma (Figs 4, *D* and 5). This enables verification of BBB closure and signifies permeability of the blood-meningeal barrier in the perivenous region, in the same distribution as the perivenular enhancement visualized at BBB opening. This blood-meningeal barrier leakiness was transitory and was observed for 24–48 hours before complete spontaneous resolution within 1 week in all participants. The observed spatiotemporal pattern of perivenular contrast enhancement is summarized in Figures 4 and 6.

Safety Evaluation

No evidence of signal dropout on T2* gradient-echo images suggestive of hemorrhage was identified in the parenchyma or extraparenchymal spaces (Fig 2, *F*). No restricted diffusion or T2-weighted FLAIR hyperintensities developed in the brain parenchyma to suggest infarct, edema, demyelination, or gliosis. There was no mass effect. Volumetric analysis of the hippocampi and entorhinal cortex documented stable cortical and white matter volumes within these treated brain regions, with no alteration relative to baseline values and compared with the untreated contralateral structures. T1 signal intensity returned to baseline at all treatment sites, with no findings to suggest parenchymal or extraparenchymal gadolinium retention or myelin loss. Study participants remained stable at follow-up neurologic and neuropsychologic examinations, with no clinical deterioration after 19 months (16 months for participant 2, 12 months for participant 3) after completion of therapy.

Discussion

Alzheimer disease (AD) drug discovery has focused on administration of exogenous monoclonal antibodies to target amyloid-β peptide. Repeated phase III clinical trial failures highlight the need for innovative therapeutic approaches, as well as improved understanding of disease pathogenesis. Focused ultrasound–induced blood-brain barrier (BBB) opening mitigates amyloid loads and improves cognitive performance in rodent models (6,7); however, the biologic mechanism for cognitive enhancement observed experimentally is unknown. Alterations in immune activity and glymphatic function have been proposed (7,13). In this study, physiologic effects of focused ultrasound–induced BBB opening were investigated and

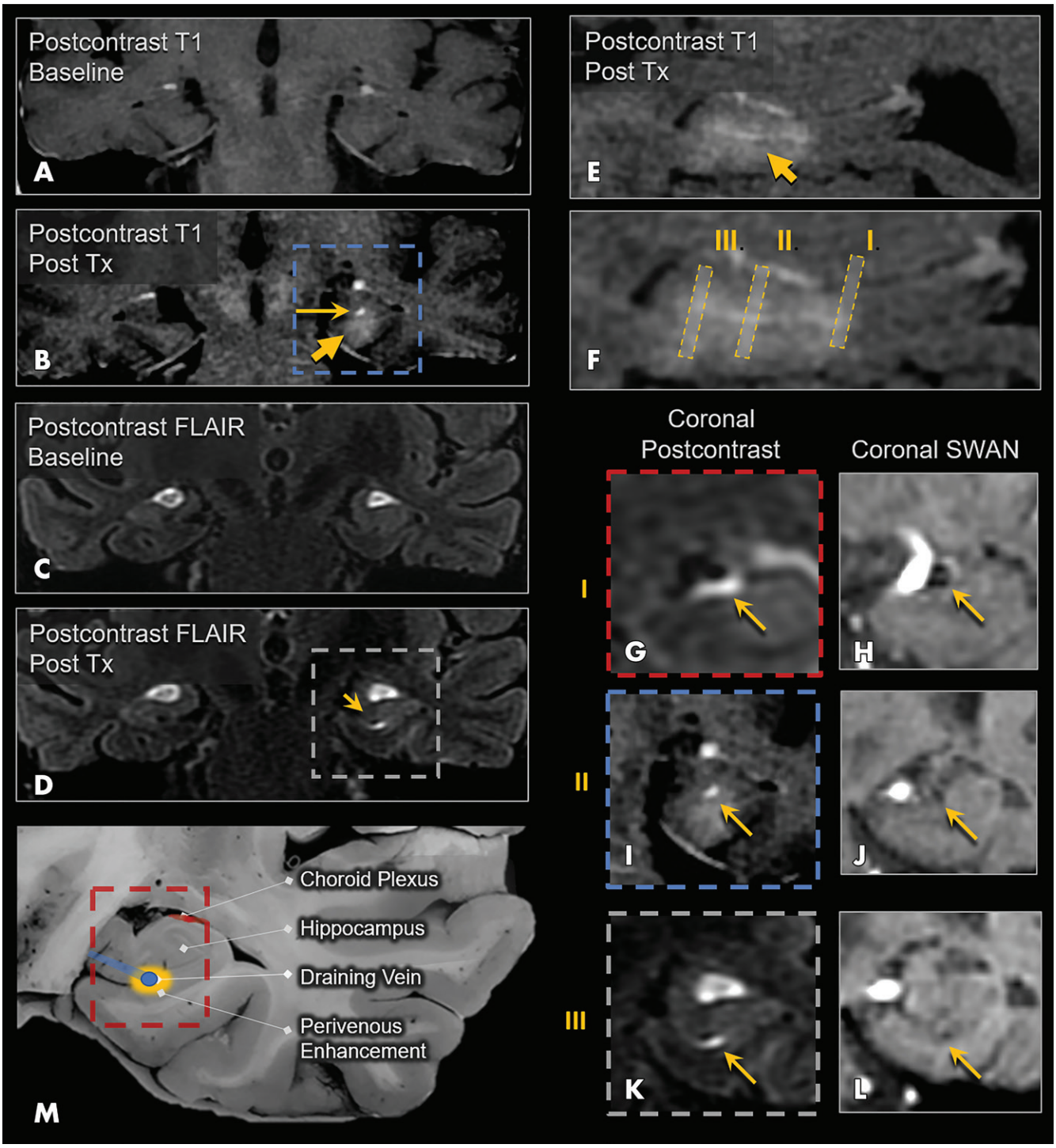

Figure 3: Perivenular enhancement pattern observed immediately after treatment (Tx) in a 72-year-old woman with Alzheimer disease. *A*, Coronal postcontrast T1-weighted MRI scan at baseline and, *B*, coronal postcontrast T1-weighted MRI scan obtained immediately after treatment show parenchymal contrast enhancement in the hippocampus and entorhinal cortex (short arrow), as well as a more avid focus of enhancement in the hippocampal fissure along the course of the hippocampal sulcus vein (long arrow). Coronal postcontrast fluid-attenuated inversion recovery (FLAIR) MRI scans at, *C*, baseline and, *D*, immediately after treatment show perivenous enhancement (arrow) around the intrahippocampal sulcal vein. *E*, Sagittal postcontrast T1-weighted MRI scan obtained immediately after treatment shows parenchymal and intense linear perivenular enhancement in the hippocampal fissure. *F*, Zoomed-in version of *E* shows coronal levels I, II, and III. *G*, Coronal postcontrast FLAIR MRI scan at the level of the basal vein of Rosenthal shows patent venous lumen with surrounding ringlike perivenous enhancement (arrow). *H*, Coronal susceptibility-weighted MRI (SWI) scan shows the basal vein of Rosenthal. *I*, Coronal postcontrast T1-weighted MRI scan at the level of the hippocampal sulcus vein shows contrast enhancement surrounding the vein. *J*, Coronal SWI scan shows the hippocampal sulcus vein (arrow) as a small black dot. *K*, Coronal postcontrast FLAIR MRI scan at the level of the intrahippocampal sulcal vein shows comma-shaped contrast enhancement surrounding this small vein. *L*, Coronal SWI scan shows the intrahippocampal sulcal vein. *M*, Schematic image shows the perivenular enhancement pattern, which was observed on immediate posttreatment images in all three participants who underwent treatment. SWAN = T2* susceptibility-weighted angiography.

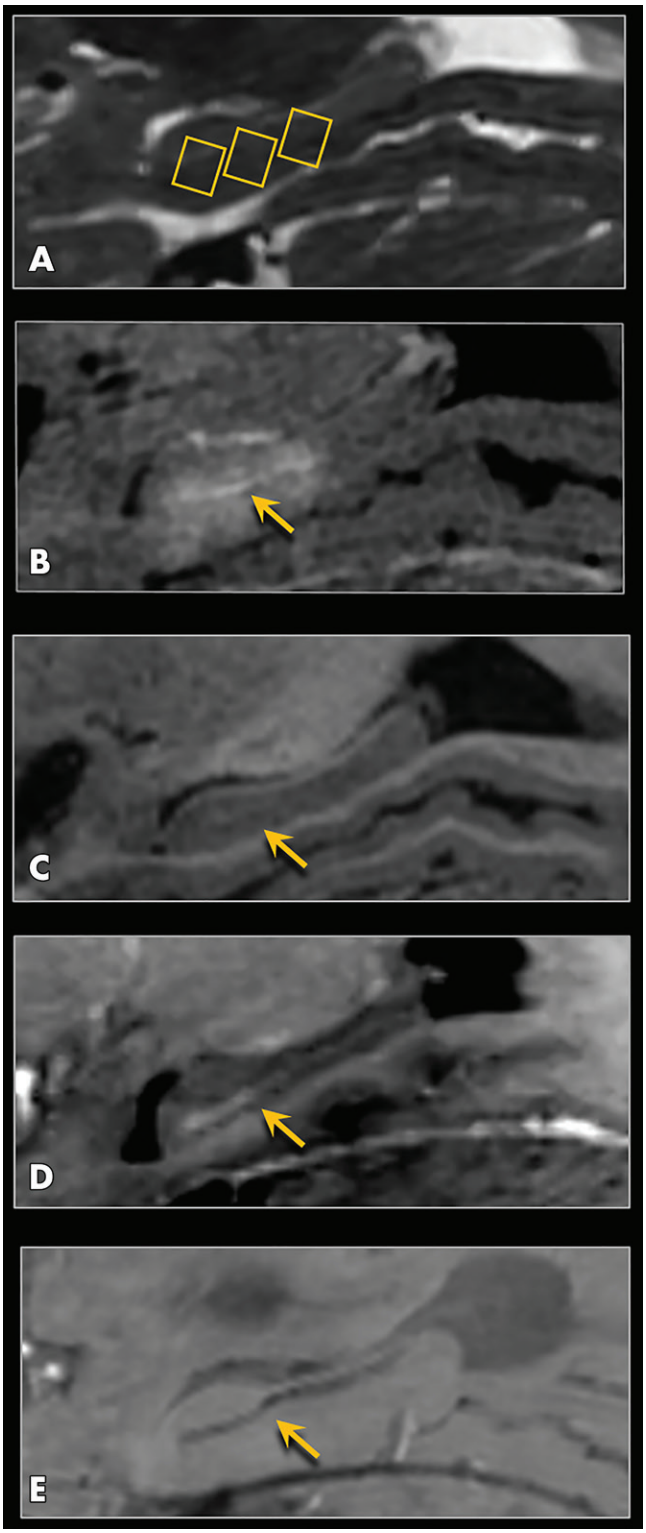

Figure 4: MRI scans show spatiotemporal pattern of perivenular enhancement in a 73-year-old woman with Alzheimer disease. *A,* Sagittal T2-weighted pretreatment image shows three selected target sites within the hippocampus (rectangles). *B,* Sagittal postcontrast T1-weighted image immediately after treatment shows parenchymal contrast enhancement within the targeted hippocampus and entorhinal cortex, as well as more hyperintense linear enhancement within the hippocampal fissure (arrow) longitudinally along the course of the hippocampal veins. *C,* Sagittal precontrast T1-weighted image obtained 24 hours after treatment shows clearance of gadolinium-containing contrast material from both the interstitial and the perivenous and perivascular spaces (arrow). *D,* Sagittal postcontrast T1-weighted image obtained 24 hours after treatment shows perivenular enhancement within the hippocampal fissure (arrow) along the course of the veins, indicating perivenous blood–meningeal barrier permeability. There is no parenchymal enhancement at this time point because of closure of the blood-brain barrier. *E,* Sagittal minimal intensity projection image obtained by using axial T2* susceptibility-weighted angiographic imaging data shows the course of hippocampal veins, which appear as a linear dark stripe within the hippocampal fissure (arrow). Perivenous enhancement seen in *B* and *D* paralleled the course of these veins, as further shown in Figure 5.

were notably found to induce a reproducible spatiotemporal contrast enhancement pattern around draining venous structures, consistent with blood-meningeal barrier permeability. This finding suggests modulation of neuroimmune response along the perivenous glymphatic efflux pathways after focused ultrasound therapy in individuals with AD.

The glymphatic pathway is a system of intracranial bulk fluid movement that functions as a waste clearance mechanism for the mammalian brain (14). By way of this system, which is facilitated by astrocytic aquaporin-4 water channels, fluid is transported from periarterial spaces through the brain interstitium to drain along perivenous spaces before exiting the cranium (14). This flow pathway, which has been intensively studied in rodents, facilitates clearance of proteins and toxic waste molecules, including amyloid-β (14,15). Available evidence suggests that such a system may be active in humans. A clinical MRI investigation using intrathecally administered gadobutrol showed that contrast material was redistributed from the subarachnoid space into the brain via transport along the course of penetrating cortical vessels, similar to experimental findings (16). A separate MRI study of individuals with idiopathic normal-pressure hydrocephalus proposed abnormal glymphatic influx and clearance kinetics (17). These investigations assessed glymphatic flow by using intrathecally administered cerebrospinal fluid tracer but did not definitively assess interstitial clearance pathways. The fate of accumulated perivenous drainage has also been elusive in experimental models because of diminutive size of rodent vasculature and limitations of two-photon microscopy in interrogation of deep brain structures.

Postcontrast brain imaging after targeted BBB opening provides a unique opportunity to assess physiology of fluid movement in the brains of individuals with AD. As we demonstrated, gadobutrol (molecular weight, 550 Da) pooled in perivenular spaces after hippocampal BBB opening to surround cortical veins and the basal vein of Rosenthal. Our findings support the glymphatic hypothesis (14) and corroborate findings by Meng et al (18), who recently showed perivenous enhancement extending toward the dural venous sinuses after focused ultrasound–induced BBB opening in various brain regions. Prolonged tracer accumulation in the perivenous space (ie, at 24 hours) has not been observed in animal models and does not support glymphatic bulk flow kinetics. Delayed perivenous enhancement was attributed to potential retrograde flow of tracer in the periarterial and subarachnoid spaces by Meng et al (18).

In consideration of proven effects of BBB manipulation and given our results, an alternate hypothesis is likely. Transient BBB opening would be expected to cause localized physiologic

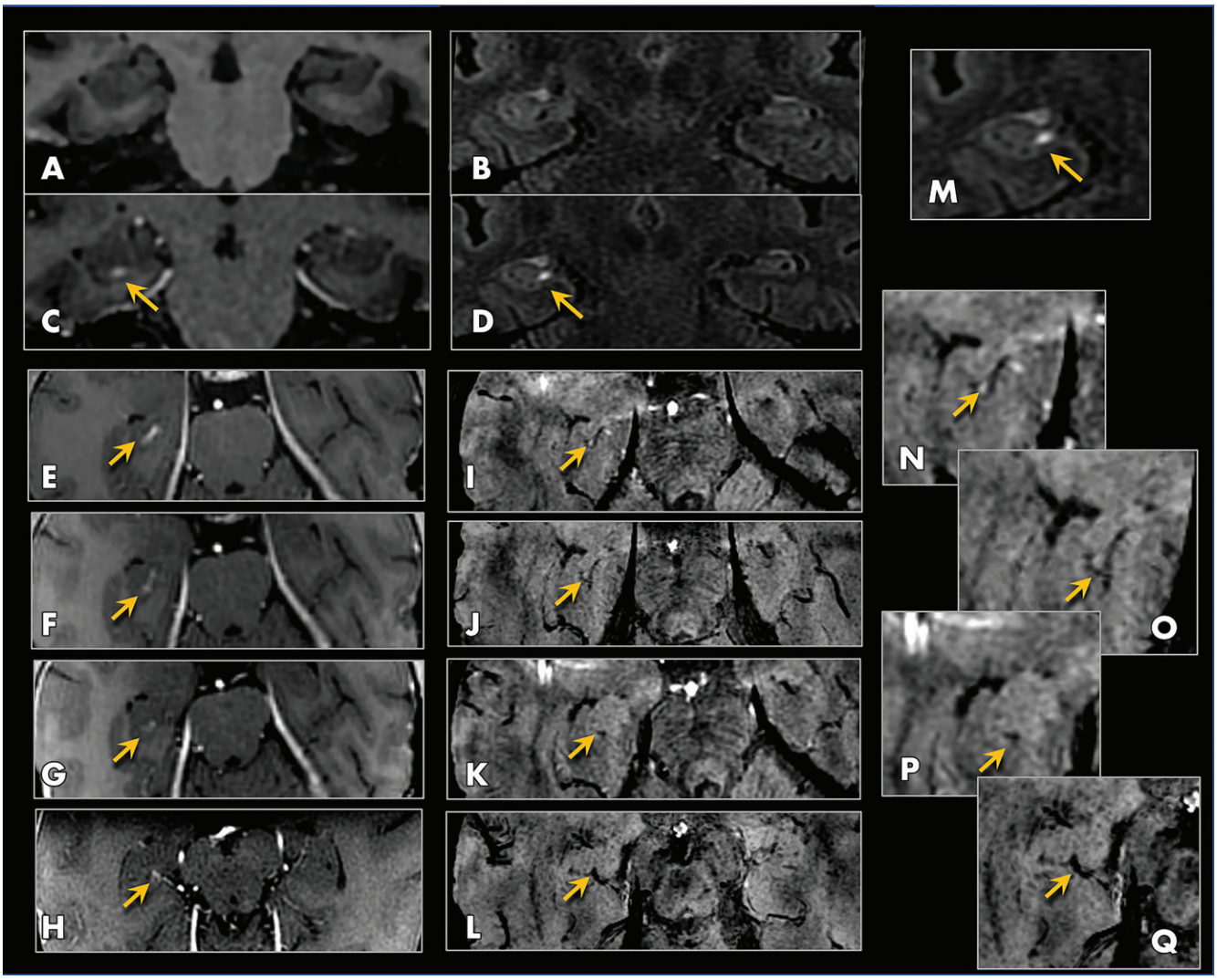

Figure 5: MRI scans show perivenular enhancement after gadobutrol clearance and blood-brain barrier (BBB) closure at 24 hours after treatment in a 61-year-old woman with Alzheimer disease. Precontrast coronal, *A*, T1-weighted and, *B*, fluid-attenuated inversion recovery (FLAIR) images, both obtained 24 hours after treatment (at same time point as Fig 3, *C*), show absence of contrast enhancement in the hippocampus and perivascular space after BBB closure. Postcontrast coronal, *C*, T1-weighted and, *D*, FLAIR images, both obtained 24 hours after treatment, show enhancement along the course of the hippocampal sulcal vein (arrows). This enhancement, shown on serial axial T1-weighted sections in, *E–H* (arrows), was present longitudinally along the course of the hippocampal veins and could be followed posteriorly to the basal vein of Rosenthal *(H)*. *I–L*, T2* susceptibility-weighted angiography (SWAN) images, corresponding to the same levels as *E–H*, show blooming susceptibility effects of the hippocampal venous structures (arrows) from the same participant, coinciding with the region of linear enhancement. This perivenous enhancement indicates blood–meningeal barrier permeability and occurred transiently after treatment before complete resolution at all treated sites. *M*, Same area as in *D*, zoomed on the right hippocampus, shows perivenous enhancement (arrow). *N–Q*, Zoomed axial SWAN images *(I–L)* show the hippocampal venous structures (arrows).

changes, including insudation at treatment sites, as occurs with BBB opening in the setting of acute focal ischemic stroke. Infiltration of plasma proteins, serum, and other intravascular contents would normally induce a secondary neuroimmunologic response. Moreover, the perivascular space is an important site of waste and neuroimmune processing (15,19). The proposed role of the perivenous space is not well characterized in humans, however. Our data demonstrate leakage of contrast material into perivenous spaces after documented BBB closure and contrast agent clearance. This indicates that delayed perivenous gadobutrol accumulation does not originate from the proximal interstitial or perivascular compartments, nor does it originate from retrograde flow from the subarachnoid space, given that precontrast images from the same time point showed no retained contrast material in these regions. Our interpretation of this imaging phenomenon, which differs from the analysis of Meng et al (18), is supported with posttreatment MRI data obtained from all three study participants. These data confirmed clearance of contrast material from the interstitium and perivascular spaces at 24 hours after treatment. Reappearance of perivenular but not parenchymal enhancement after repeated contrast material administration at 24 hours after treatment suggests a distinct cause for the observed localized perivenular contrast material accumulation. This observation may be biologically important and can be explained by transient development of perivenous permeability of the blood-meningeal barrier. The thin-walled cerebral meningeal venules and veins, which lack endothelial tight junctions, are the primary sites of leukodiapedesis into the central

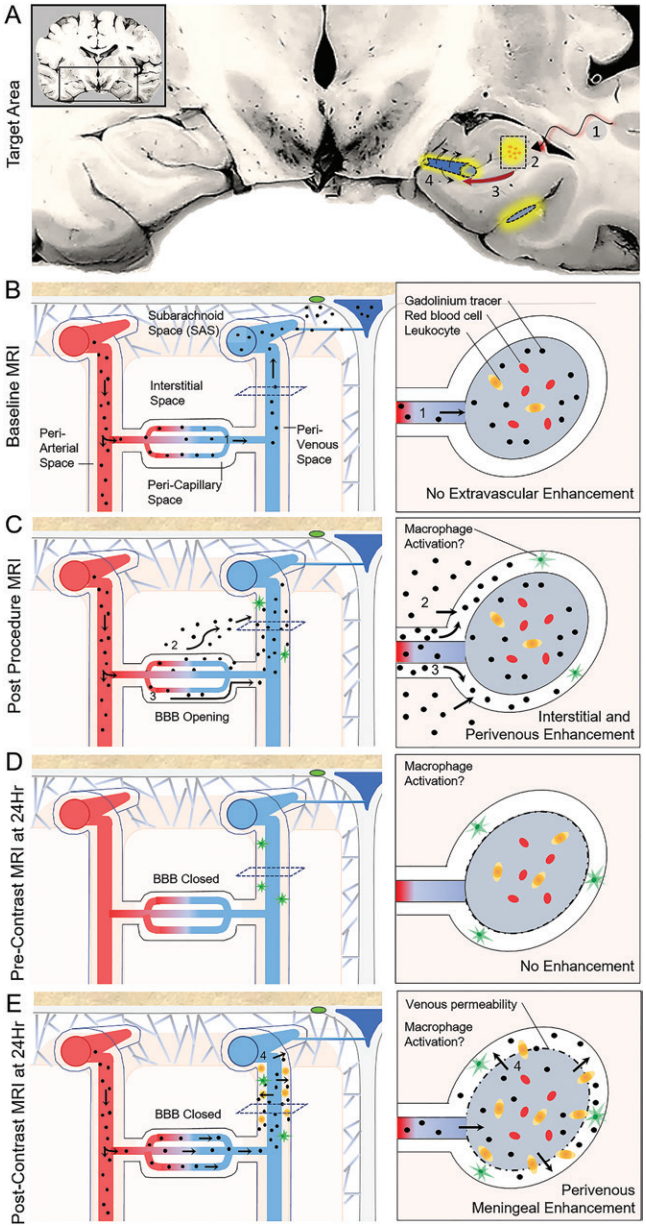

Figure 6: Observed tracer movement pattern after focused ultrasound-induced blood-brain barrier (BBB) opening and proposed glymphatic efflux route in humans. *A*, Coronal schematic view through the temporal lobes summarizes procedural effects of BBB opening. *1*, Focused ultrasound energy was delivered, along with intravenous microbubbles, to the hippocampal target site (boxed area). *2*, Contrast extravasation from capillaries into the interstitial space (yellow) indicates BBB opening within the targeted volume. *3*, Contrast material flows downstream from the interstitial space to the perivenular space, along the proposed glymphatic efflux route, resulting in perivenous enhancement. *4*, Reactive venous permeability is proposed to account for contrast material leakage into the perivenous sheath, suggesting a physiologic perivenular neuroimmune reaction. *B*, Normal flow of contrast material during baseline homeostatic state. With closed (intact) BBB, contrast material travels through the intravascular compartment and exits the cranial cavity via the dural venous sinuses and along the dura. *C*, Flow of contrast material during focused ultrasound–induced BBB opening. Because of acquired permeability of the capillary walls, gadobutrol extravasates from the intravascular compartment into the pericapillary or interstitial space and flows downstream to perivenous spaces. *D*, At 24 hours after treatment, precontrast images demonstrate gadolinium clearance from both the brain parenchyma and perivascular spaces due to rapid transit related to bulk fluid and solute flow. *E*, Postcontrast imaging at 24 hours after focused ultrasound. Notably, after repeat intravenous gadobutrol administration, no intraparenchymal contrast enhancement is seen because of closure of the BBB. However, gadolinium-based contrast agent accumulation reappears around the draining veins, suggesting permeability of the postcapillary venules and meningeal veins.

nervous system (20). In vivo microscopy in animal models of Alzheimer disease have demonstrated that proinflammatory molecules promote leukocyte adhesion and entry around venules (21). Thus, future experimental work investigating cellular, molecular, and histologic changes occurring in the perivenous space is warranted to further elucidate this clinical physiologic imaging marker, which is likely related to immune cell trafficking (15,20,21).

Limitations of this study included a small sample size of three participants who underwent treatment at one institution and were part of the ongoing multicenter trial. In addition, the studied cohort consisted of only female participants. Understanding the response of patients with AD relative to that of healthy, young, age-matched control participants may be addressed in future experimental work and would help elucidate the physiologic phenomena associated with focused ultrasound treatment discussed here.

On the basis of this study, we conclude that MRI-guided focused ultrasound administered in combination with intravascular microbubbles results in transient spatially precise blood-brain barrier (BBB) opening within the hippocampus and entorhinal cortex in individuals with Alzheimer disease (AD). Contrast-enhanced MRI revealed a unique contrast enhancement pattern, suggesting a perivenous glymphatic efflux route in humans and functional meningeal venous wall changes resulting in permeability of the blood-meningeal barrier. Further investigation is needed to elucidate the biologic importance of this imaging marker and how this phenomenon resulting from focused ultrasound–induced BBB opening relates to modulation of amyloid-β levels and cognitive function in AD.

Author contributions: Guarantor of integrity of entire study, Rashi I. Mehta; study concepts/study design or data acquisition or data analysis/interpretation, all authors; manuscript drafting or manuscript revision for important intellectual content, all authors; approval of final version of submitted manuscript, all authors; agrees to ensure any questions related to the work are appropriately resolved, all authors; literature research, Rashi I. Mehta, Rupal I. Mehta, A.R.R.; clinical studies, Rashi I. Mehta, J.S.C., M.W.H., M.R., U.N., P.W., A.R.R.; experimental studies, Rashi I. Mehta, J.S.C., M.R., U.N., P.F.D., A.R.R.; statistical analysis, Rashi I. Mehta, P.W., P.F.D., A.R.R.; and manuscript editing, all authors

Disclosures of Conflicts of Interest: **Rashi I. Mehta** disclosed no relevant relationships. **J.S.C.** disclosed no relevant relationships. **Rupal I. Mehta** disclosed no relevant relationships. **M.W.H.** Activities related to the present article: institution received a contract to conduct the study from Insightec. Activities not related to the present article: gave lectures for Medtronic and Anthem. Other relationships: disclosed no relevant relationships. **M.R.** disclosed no relevant relationships. **U.N.** disclosed no relevant relationships. **P.L.** disclosed no relevant relationships. **P.W.** disclosed no relevant relationships. **P.F.D.** disclosed no relevant relationships. **A.R.R.** Activities related to the present article: disclosed no relevant relationships. Activities not related to the present article: is on the board of Sollis Therapeutics and Avation Medical; is a consultant for Sollis Therapeutics, Avation Medical, and Neurotechnology Innovations Management; . Other relationships: disclosed no relevant relationships.

References

1. Reitz C, Brayne C, Mayeux R. Epidemiology of Alzheimer disease. Nat Rev Neurol 2011;7(3):137–152.

2. Leading Causes of Death. Centers for Disease Control and Prevention. https://www.cdc.gov/nchs/fastats/leading-causes-of-death.htm. Published 2020. Accessed December 21, 2020.
3. Perl DP. Neuropathology of Alzheimer's disease. Mt Sinai J Med 2010;77(1):32–42.
4. Cummings J, Feldman HH, Scheltens P. The "rights" of precision drug development for Alzheimer's disease. Alzheimers Res Ther 2019;11(1):76.
5. van Dyck CH. Anti-amyloid-β monoclonal antibodies for Alzheimer's disease: pitfalls and promise. Biol Psychiatry 2018;83(4):311–319.
6. Jordão JF, Ayala-Grosso CA, Markham K, et al. Antibodies targeted to the brain with image-guided focused ultrasound reduces amyloid-beta plaque load in the TgCRND8 mouse model of Alzheimer's disease. PLoS One 2010;5(5):e10549.
7. Jordão JF, Thévenot E, Markham-Coultes K, et al. Amyloid-β plaque reduction, endogenous antibody delivery and glial activation by brain-targeted, transcranial focused ultrasound. Exp Neurol 2013;248:16–29.
8. Burgess A, Dubey S, Yeung S, et al. Alzheimer disease in a mouse model: MR imaging-guided focused ultrasound targeted to the hippocampus opens the blood-brain barrier and improves pathologic abnormalities and behavior. Radiology 2014;273(3):736–745.
9. Scarcelli T, Jordão JF, O'Reilly MA, Ellens N, Hynynen K, Aubert I. Stimulation of hippocampal neurogenesis by transcranial focused ultrasound and microbubbles in adult mice. Brain Stimul 2014;7(2):304–307.
10. Burgess A, Ayala-Grosso CA, Ganguly M, Jordão JF, Aubert I, Hynynen K. Targeted delivery of neural stem cells to the brain using MRI-guided focused ultrasound to disrupt the blood-brain barrier. PLoS One 2011;6(11):e27877.
11. Lipsman N, Meng Y, Bethune AJ, et al. Blood-brain barrier opening in Alzheimer's disease using MR-guided focused ultrasound. Nat Commun 2018;9(1):2336.
12. McKhann GM, Knopman DS, Chertkow H, et al. The diagnosis of dementia due to Alzheimer's disease: recommendations from the National Institute on Aging-Alzheimer's Association workgroups on diagnostic guidelines for Alzheimer's disease. Alzheimers Dement 2011;7(3):263–269.
13. Lee Y, Choi Y, Park EJ, et al. Improvement of glymphatic-lymphatic drainage of beta-amyloid by focused ultrasound in Alzheimer's disease model. Sci Rep 2020;10(1):16144.
14. Iliff JJ, Wang M, Liao Y, et al. A paravascular pathway facilitates CSF flow through the brain parenchyma and the clearance of interstitial solutes, including amyloid β. Sci Transl Med 2012;4(147):147ra111.
15. Mestre H, Kostrikov S, Mehta RI, Nedergaard M. Perivascular spaces, glymphatic dysfunction, and small vessel disease. Clin Sci (Lond) 2017;131(17):2257–2274.
16. Ringstad G, Valnes LM, Dale AM, et al. Brain-wide glymphatic enhancement and clearance in humans assessed with MRI. JCI Insight 2018;3(13):e121537.
17. Ringstad G, Vatnehol SAS, Eide PK. Glymphatic MRI in idiopathic normal pressure hydrocephalus. Brain 2017;140(10):2691–2705.
18. Meng Y, Abrahao A, Heyn CC, et al. Glymphatics visualization after focused ultrasound-induced blood-brain barrier opening in humans. Ann Neurol 2019;86(6):975–980.
19. Brown R, Benveniste H, Black SE, et al. Understanding the role of the perivascular space in cerebral small vessel disease. Cardiovasc Res 2018;114(11):1462–1473.
20. Krahn V. Leukodiapedesis and leukocyte migration in the leptomeninges and in the subarachnoid space. J Neurol 1981;226(1):43–52.
21. Michaud JP, Bellavance MA, Prefontaine P, Rivest S. Real-time in vivo imaging reveals the ability of monocytes to clear vascular amyloid beta. Cell Rep. 2013;14;5(3):646–653.